

In situ observation of individual variant transformations in polycrystalline NiTi

S.L. Raghunathan, M.A. Azeem, D. Collins and D. Dye*

Department of Materials, Imperial College London, London SW7 2AZ, UK

Received 30 June 2008; revised 9 July 2008; accepted 10 July 2008

Available online 18 July 2008

The transformation behaviour of the individual texture components of NiTi rolled sheet was examined by synchrotron X-ray diffraction. The diffraction measurements performed in this study only captured a small fraction of orientation space, allowing the transformation of individual orientations to be studied. It was found that the individual B2 orientations transform at distinct points in the load plateau and that this can be correlated with the appearance of individual B19' variant orientations.

© 2008 Acta Materialia Inc. Published by Elsevier Ltd. All rights reserved.

Keywords: Shape memory alloys (SMA); Synchrotron radiation; Martensitic phase transformation; Texture; Variant selection

NiTi-based shape memory alloys are of great current interest in the aerospace industry as potential candidates for replacing mechanical actuators. The operating principle is to exploit the phase transformation to achieve a change in shape of the sample, which occurs due to a combination of temperature and stress. In NiTi the high-temperature austenite phase is an ordered B2 structure, whilst the low-temperature phase is monoclinic B19' martensite. These two phases have been shown [1–3] to possess a $\{110\}_{B2} \parallel (002)_{B19'}$ or $\{110\}_{B2} \parallel (11\bar{1})_{B19'}$ orientation relationship. It is possible for an intermediate phase to form during the transformation pathway, either R or B19, depending on the prior thermomechanical processing or alloying additions [4]. The understanding of variant selection processes during deformation is critical to the successful modelling of phase transformations [5–8].

Previous researchers [9] have shown using microscopy that the transformation is progressive within a single grain, proceeding via the selection of twin-related variants that accommodate the imposed strain along the tensile axis and also self-accommodate the off-axis transformation strains [10–12]. Also, before-and-after texture analysis has shown [13], at least empirically, how the texture evolves during loading to the B19' state and unloading back to the B2 phase. Finally, Vaidyanathan and co-workers [14–18] performed in situ neutron

diffraction using the large area detectors at NPD and SMARTS and showed that, measured over a large fraction of orientation space, the transformed volume fraction varies with the overall transformation strain in the load plateau region.

In this paper, results of a synchrotron diffraction study carried out at the European Synchrotron Research Facility (ESRF) are presented. These are used to examine the progress of the transformation for a small fraction of orientation space, allowing the observation of the transformation of an individual component of the starting B2 texture.

Dogbone-shaped tensile specimens of NiTi sheet were loaded in tension at room temperature using a FaME38 electro-thermomechanical tester while in situ X-ray synchrotron diffraction was performed on the ID15B beamline at ESRF. Figure 1a shows a side view of the diffraction geometry. Diffraction patterns were collected every 4 s using an incident X-ray wavelength of 0.1415 Å and a Pixium area detector. The diffraction rings collected (Fig. 1b) give information about the response of grains satisfying the Bragg condition, with $\psi = 0^\circ$ corresponding to the tensile axis of the test, also the rolling direction (RD) of the sheet and $\psi = 90^\circ$ corresponding to the normal direction (ND) of the rolled sheet employed. The rings were segmented into 10° regions using the software program FIT2D [19]. Peaks were indexed using GSAS [20] (Fig. 1c). R-phase as well as the expected B2 phase was determined to be present at the beginning of the test. The diffraction spectra were fitted

* Corresponding author. Tel.: +44 20 7594 6811; fax: +44 20 7594 6758; e-mail: david.dye@imperial.ac.uk

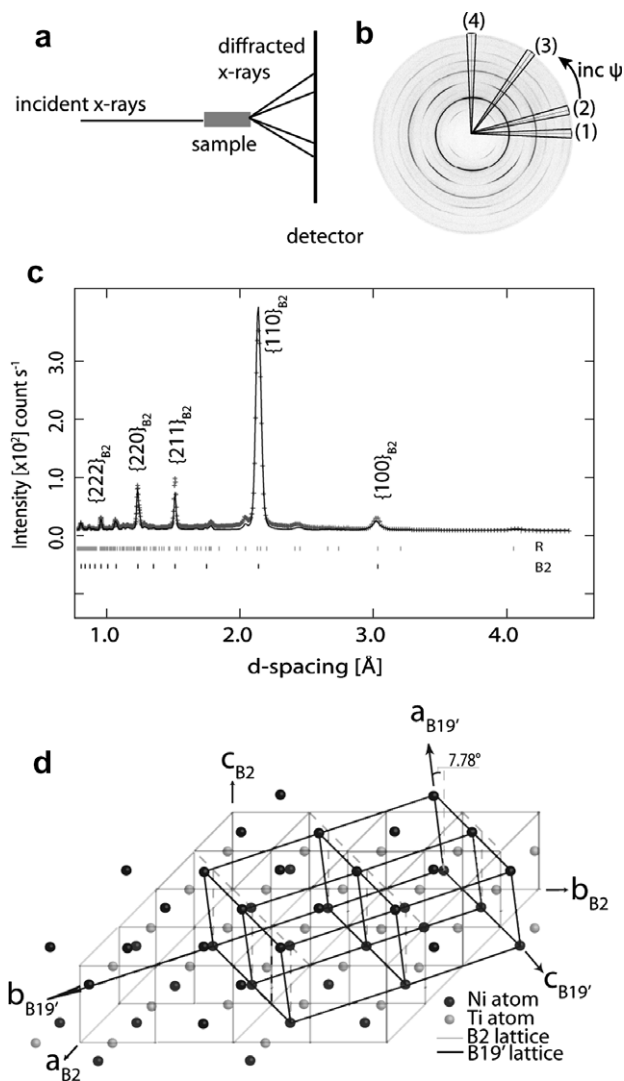


Figure 1. (a) Schematic (side view) of the diffraction geometry. (b) Resultant Debye–Scherrer diffraction rings at the beginning of the test. Azimuthal segments indicated are (1) $-5^\circ < \psi < 5^\circ$ (RD), (2) $15^\circ < \psi < 25^\circ$, (3) $55^\circ < \psi < 65^\circ$ and (4) $85^\circ < \psi < 95^\circ$ (ND). (c) Synchrotron diffraction spectrum of the starting sample. (d) The unit cell relationships between the B2 and B19' phases.

using a peak-fitting script developed by S.S. Babu. These fitted intensities were subsequently normalised for each phase; Figure 1d shows a schematic of the predominant orientation relationship between the B2 and B19', i.e. $\{110\}_{B2} \parallel \{110\}_{B19'} \parallel (002)_{B19'} \parallel (002)_{B2}$.

The changes in intensity around the diffraction rings in Figure 1b give an indication that a rolling texture is present in the NiTi sheet. The B2 phase is expected to deform by $\langle 111 \rangle$ slip and pencil glide, and therefore this observed texture is not unreasonable.

The measured composition of the sample tested was found to be 52.9 at.% Ni, 47.1 at.% Ti with 0.05 at.% O. The transformation temperatures were measured using differential scanning calorimetry (DSC) and the A_f and M_f temperatures were found to be ~ 50 and -80°C , respectively.

In Figure 2 the macroscopic stress–strain response of the NiTi is shown. The shape memory behaviour

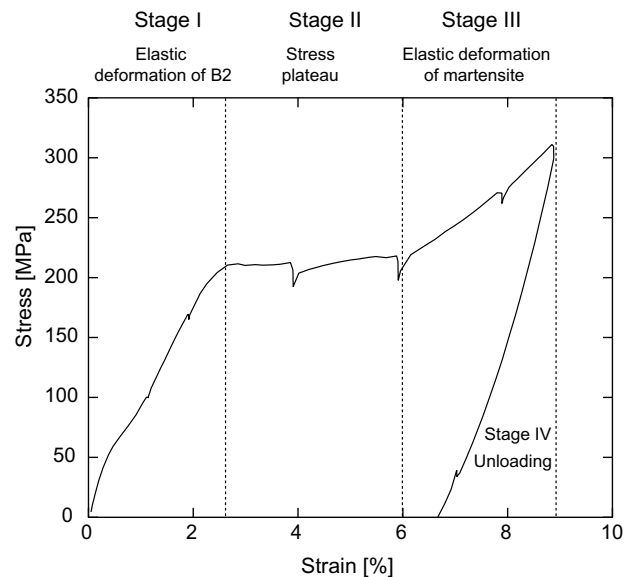


Figure 2. Macroscopic stress–strain response of NiTi. Stage I represents in initial elastic loading of the B2 phase; Stage II indicates the stress-plateau regime; Stage III is the regime for martensitic elastic deformation; and Stage IV is unloading at the end of the test.

observed is as expected: an initial elastic regime until a strain of $\sim 2.2\%$ followed by a stress plateau regime until a strain of $\sim 6\%$. The stress was then increased to 300 MPa before unloading. The sample did not show complete strain recovery as the test temperature was lower than A_f [21]. The load drops correspond to position holds during the test.

Figure 3 shows the spectral evolution in the d -spacing range of 1.9–2.4 Å at the selected azimuthal segments shown in Figure 1b and Figure 4b shows the evolution of the fitted normalised intensities. In general, the intensities of the B2 and B19' show a gradual change initially in Stage II, clearly evident in Figure 4b, culminating with a sudden change in intensity at the end. Along the RD in the plateau regime, the intensity of $\{110\}_{B2}$ peak does not change substantially until the end of the stress plateau where a large decrease is observed. At the same point in the measurement sequence the intensity of $(002)_{B19'}$ increases suddenly in the RD. Along the ND, the initial $\{110\}_{B2}$ intensity is lower compared to that of the RD. During Stage II the $(020)_{B19'}$ peak appears as a shoulder at the expense of the $\{110\}_{B2}$ peak. In Figure 3c ($55^\circ < \psi < 65^\circ$ from the RD), the appearance of the $(012)_{B19'}$ peak is observed during Stage II as well as a small fraction of $(002)_{B19'}$. However, at $15^\circ < \psi < 25^\circ$ from the RD (Fig. 3d), the appearance of the $(11\bar{1})_{B19'}$ is observed. For the $(11\bar{1})_{B19'}$ and $(012)_{B19'}$ peaks, it was not possible to determine which parent B2 variants they transformed from, purely due to the small region of the orientation space being measured.

The diffraction measurements performed in this study only capture a small fraction of orientation space lying along the periphery of the overall texture pole figure due to the low intrinsic divergence of the synchrotron beam utilised ($< 1^\circ$). This allows the transformation of individual orientations in the polycrystal to be studied,

Download English Version:

<https://daneshyari.com/en/article/1502221>

Download Persian Version:

<https://daneshyari.com/article/1502221>

[Daneshyari.com](https://daneshyari.com)